Astron. Astrophys. 341, 256–263 (1999)

ASTRONOMY AND ASTROPHYSICS

Dense gas in nearby galaxies⋆

XII. A survey for CO $J = 3 - 2$ emission

R. Mauersberger[1], **C. Henkel**[2], **W. Walsh**[3], **and A. Schulz**[4,5]

[1] Steward Observatory, The University of Arizona, Tucson, AZ 85721, USA
[2] Max-Planck-Institut für Radioastronomie, Auf dem Hügel 69, D-53121 Bonn, Germany
[3] Radioastronomisches Institut der Universität Bonn, Auf dem Hügel 71, D-53121 Bonn, Germany
[4] Institut für Physik und Didaktik, Universität zu Köln, Gronewaldstrasse 22, D-50931 Köln, Germany
[5] Institut für Astrophysik und Extraterrestrische Forschung, Universität Bonn, Auf dem Hügel 71, D-53121 Bonn, Germany

Received 27 July 1998 / Accepted 18 September 1998

Abstract. The $J = 3 - 2$ sub-mm line of ^{12}CO has been observed with the Heinrich-Hertz-Telescope (HHT) toward a sample of 28 nearby galaxies, and toward Arp 220. All sources are detected. This is the largest extragalactic sample of CO $3 - 2$ spectra published so far. The $3 - 2$ line fluxes, I_{32}, are compared to $1 - 0$ and $2 - 1$ fluxes measured with the IRAM 30-m telescope. Model calculations show that the I_{32}/I_{10} ratio can be used as a measure of the average H_2 density. For most sources observed, I_{32}/I_{10} is in the range 0.2–0.7, which is predicted if kinetic temperatures are < 50 K and/or H_2 densities $< 1000\,\mathrm{cm}^{-3}$.

Our measurements of the $J = 1 - 0$, $2 - 1$, and $3 - 2$ lines toward M 82 do not support earlier claims of $2 - 1/1 - 0$ line ratios much larger than 1. As in other active galaxies (NGC 253, Arp 220) the measured line intensity ratio is close to unity. Unlike single dish data from the lower excited CO lines, the CO $3 - 2$ profile toward Arp 220 shows two velocity components, possibly arising from the edges of its molecular disk.

Key words: radio lines: galaxies – galaxies: spiral – galaxies: ISM – galaxies: general – ISM: molecules – surveys

1. Introduction

Low lying rotational transitions of CO at mm-wavelengths are widely used as tracers of molecular hydrogen. This is valid for clouds in the Galactic disk, the Galactic center and also for extragalactic objects (e.g. Strong et al. 1988, Bitran et al. 1997, Mauersberger et al. 1996b). To date, however, the widespread use of CO $J = 1 - 0$ and $2 - 1$ spectroscopy (e.g. Young et al. 1995, Braine et al. 1993, Sage 1993, Chini et al. 1996 and Elfhag et al.1996) is not complemented by a systematic survey for higher rotational CO transitions (for a few exceptions, see Steppe et al. 1990, Tilanus et al. 1991, Güsten et al. 1993, White et al. 1994, Israel et al. 1995, Mauersberger et al. 1996a), so that important aspects of molecular excitation emphasizing warmer and denser molecular regions remain virtually unexplored.

The $J = 1$ and 2 levels of CO are 5.5 and 17 K above the ground level. The $J = 3$ state, however, is at 33 K, and hence traces a warmer gas component that may not be pervasive in galactic disks, but which is certainly important toward the central regions of galaxies, particularly toward the more active ones. In addition, the "critical density" of the CO $J = 3 - 2$ transition (at which collisional excitation matches spontaneous decay in the optically thin case) is $\sim 10^5\,\mathrm{cm}^{-3}$, vs. 10^3 and $10^4\,\mathrm{cm}^{-3}$ for the two lower transitions.

We have used the Heinrich-Hertz Telescope on Mt. Graham to observe the CO $3 - 2$ line in a number of galaxies which are known to be strong emitters in the $J = 1 - 0$ and $2 - 1$ transitions. The main purpose is to present a sample of sources with integrated line intensities of three CO transitions and almost identical beam widths ($\sim 20''$), and to provide a starting point for extended CO $3 - 2$ surveys, either covering larger samples of sources or involving detailed maps and isotopic studies for individual sources.

2. Observations

2.1. Observations at the Heinrich-Hertz-Telescope

The observations of the ^{12}CO $3-2$ line were conducted with the 10-m Heinrich-Hertz-Telescope (for a description of the HHT, see Baars & Martin 1996) on Mt. Graham in southern Arizona during two observing sessions on December 18/19, 1997 and January 6/7 1998 under very good weather conditions. The spectrum of M 82 was measured in May 1998. The zenith optical depth at 345 GHz was in most cases 0.2; only in a few observations was it as high as 0.4. Most sources have been observed at actual optical depths $\tau < 0.6$; only for Cen A τ was 1.1. The latter source was also partially blocked by trees, so the absolute calibration of Cen A is much less secure than for the

Send offprint requests to: R. Mauersberger

⋆ Based on observations with the Heinrich-Hertz-Telescope (HHT). The HHT is operated by the Submillimeter Telescope Observatory on behalf of Steward Observatory and the MPI für Radioastronomie.

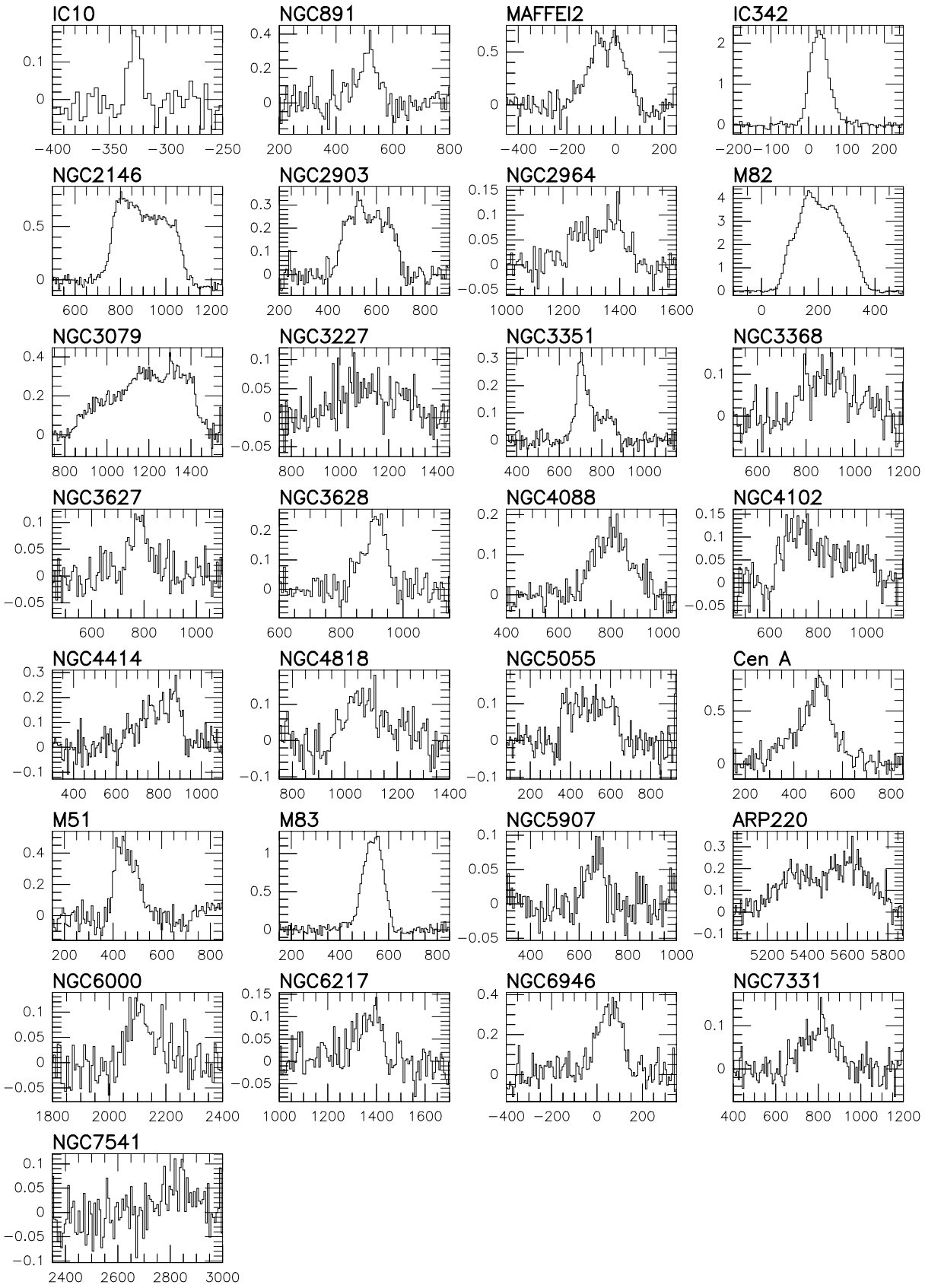

Fig. 1. ^{12}CO $(J = 3 - 2)$ spectra. The velocity scale corresponds to the Local Standard of Rest. Intensities are in K (main-beam brightness temperature)

Table 1. Line parameters of detected sources[c]

Source	α_{1950} h m s	δ_{1950} ° ′ ″	$I(1-0)$ K km s^{-1}	$I(2-1)$ K km s^{-1}	$I(3-2)$ K km s^{-1}	$v_{\rm LSR}^{\rm a}$ km s^{-1}	$\Delta v^{\rm a}$ km s^{-1}
IC 10	0 17 44.3	59 00 36	19	~ 20	2.2(0.3)	$-327(1)$	10.9(1.6)
NGC 891	2 19 23.8	42 07 10	~ 110	~ 90	24(2)	514(3)	74(9)
Maffei 2	2 38 08.5	59 23 24	100		109(4)	$-36(3)$	158(6)
IC 342	3 41 56.6	67 56 25	210	190	138(1)	27.5(0.3)	55.2(0.6)
NGC 2146	6 10 40.2	78 22 23	118	138	193[b]	902[b]	211[b]
NGC 2903	9 29 19.9	21 43 24	93	60	63(2)	561(3)	196(6)
NGC 2964	9 39 56.8	32 04 34	25	24	17(1)	1333(7)	191(14)
M 82	9 51 43.9	69 55 01	*736*	*821*	840[b]	210[b]	169[b]
NGC 3079	9 58 35.4	55 55 11	212		144[b]	1202[b]	321[b]
NGC 3227	10 20 46.8	20 07 06	54	42	16(1)	1119(14)	294(30)
NGC 3351	10 41 18.9	11 58 02	17	28	28[b]	739[b]	127[b]
NGC 3368	10 44 07.4	12 05 01	35	59	22(2)	891(11)	218(24)
NGC 3627	11 17 39.7	13 15 37	39	~ 39	8.8(1)	784(4)	80(11)
NGC 3628	11 17 41.6	13 51 40	90	~ 100	20(1)	911(2)	80(6)
NGC 4088	12 03 01.7	50 49 07	*48*		26(1)	803(3)	162(7)
NGC 4102	12 03 50.8	52 59 21	*85*		31[b]	725[b]	74[b]
NGC 4414	12 23 57.8	31 29 58	57	46	38[b]	826[b]	124[b]
NGC 4818	12 54 12.7	$-$ 8 15 13	*43*		20[b]	1077[b]	67[b]
NGC 5055	13 13 34.7	42 17 32	*70*		28(2)	497(10)	230(18)
Cen A	13 22 33.0	$-$42 45 24			130[b]	483[b]	150[b]
M 51	13 27 46.1	47 27 21	*78*		49(2)	451(2)	98(5)
M 83	13 34 11.7	$-$29 36 39			126(2)	537(1)	94(1)
NGC 5907	15 14 34.8	56 30 33	32	16	6(0.7)	668(5)	77(10)
Arp 220	15 32 47.3	23 40 06	109	~ 66	98	5516	306
NGC 6000	15 46 44.1	$-$29 14 08	*95*	11	12(2)	2114(7)	108(18)
NGC 6217	16 35 05.1	78 18 05	19	18	12.9(1.3)	1369(6)	118(14)
NGC 6946	20 33 48.0	59 59 00	68		46(2)	56(3)	124(7)
NGC 7331	22 34 46.1	34 09 08	38	19	17.5(1.2)	806(6)	166(13)
NGC 7541	23 12 12.1	4 15 46	*28*		7(1)	2823(12)	124(24)

[a] from Gaussian fit to the $3-2$ line.
[b] in the case of non-Gaussian profiles, the line flux and the median velocity and widths are computed from the moments.
[c] All $J=1-0$ and $2-1$ data are from the 30-m telescope.
References: NGC 2146, NGC 2964, NGC 3079, NGC 3351, NGC 3368, NGC 4414, NGC 5907, NGC 6217, NGC 7331: Braine et al. (1993); IC 10: Becker (1990); NGC 891: García-Burillo et al. (1992); Maffei 2, NGC 6946: Weliachew et al. (1988); IC 342: Eckart et al. (1990); NGC 2903: Jackson et al. (1991); Arp220: Solomon et al. (1990), Jackson et al. (1991); NGC 3627: Reuter et al. (1996), NGC 3628: Reuter et al. (1991), Boisse et al. (1987); NGC6000: Chini et al. (1996); data based on own measurements at the 30 m telescope are given in italics.

other sources. The atmospheric fluctuations and the atmospheric model introduce a calibration uncertainty not greater than 5%.

A 2 channel SIS receiver was equipped with a 1024 channel acousto optical spectrometer with a total bandwidth of 1 GHz. The second channel, which has a more reliable calibration, was used for this study. System temperatures for a single sideband were typically 400–1500 K ($T_{\rm MB}$). The beamwidth was $21''$. The receiver was sensitive to both sidebands. The CO line was observed in the lower sideband. Any imbalance of the gains in the lower and upper sideband will increase the calibration errors. Tuning the receiver with different parameters for the backshort resulted in variations of the intensity of IC 342 of up to $\pm 12.5\%$.

All results are given on a main-beam brightness temperature ($T_{\rm MB}$) scale. This is related to the antenna temperature via $T_{\rm MB} = (F_{\rm eff}/B_{\rm eff})T_{\rm A}^*$; it is the same calibration scheme as used at the IRAM 30-m telescope (Downes, 1989). The main-beam efficiency, $B_{\rm eff}$, has been measured by the SMTO staff in November 1997 to be 0.50 (± 0.03) toward Saturn, which at that time had a size of $18''$. The surface of the HHT is within 25μm (i.e. $\lambda/35$ at 345 GHz) very accurate. There are no strong error beams at 345 GHz. This reduces the effect of source size on the appropriate source coupling efficiency. The forward hemisphere efficiency, $F_{\rm eff}$, is close to 1. On that scale, a spectrum of the CO $J=3-2$ line taken toward IRC+10216 yields $T_{\rm MB} = 44$ K and $\int T_{\rm MB} {\rm d}v = 944\,{\rm K\,km\,s^{-1}}$. The uncertainty of $B_{\rm eff}$ introduces a 6% calibration uncertainty.

The spectra were taken using a wobbling secondary mirror with a beam throw of $\pm 4'$ in azimuth. Scans obtained with reference positions on either side were coadded to ensure flat baselines. Baselines of order zero or one were subtracted from the data. The $T_{\rm A}^*$ scale is determined by measurements of an ambient load and the sky, which are interspersed with the spec-

tral line observations. The receiver temperature was determined from measurements of an ambient load and a cold load (at liquid nitrogen temperature) after each retuning of the receiver. The variations of the sky opacity were also monitored by a tilting radiometer at 230 GHz.

Our pointing was based on the pointing measurements obtained by the SMTO staff, which gave an RMS deviation of measured pointing sources from a best model of $5''$. For a $21''$ beam, the resulting calibration uncertainty could result in an underestimate of the intensity of a point source of 18%, and less for extended sources. Although most of our observed positions should be exact within $5''$ we cannot exclude that a few sources have pointing errors as large as half a beamwidth. This would result in an underestimate of the calibration of 50%.

The calibration uncertainty resulting from the above factors (under the assumption of a $5''$ pointing error) is $\pm 23\%$, which is consistent with variations commonly observed at sub-mm wavelengths.

2.2. Observations at the IRAM 30-m telescope

Some of our sources were observed at the IRAM 30-m telescope in the $J = 1 - 0$ and $2 - 1$ transitions of ^{12}CO in May 1998. The wobbling secondary mirror was used with a beam throw of $4'$ in azimuth. Both lines were observed simultaneously using two 512×1 MHz filterbank spectrometers. The beamwidths of the 30-m telescope at 115 and 230 GHz are 21 and $12''$. Except for M 82, only the 115 GHz data were used in this paper since the incomplete sampling of our maps did not allow to obtain $2 - 1$ data convolved to a $21''$ beam.

3. Results

In Fig. 1, we show the spectra obtained toward 29 external galaxies. For the presentation, the resolution of the spectrometer has been degraded to 6.7 km s^{-1}, only for IC 10 it is 3.8 km s^{-1}. We have detected line emission toward all sources. For most of these sources, this is the first time that $J = 3 - 2$ data are published. Even for Centaurus A, which at Mount Graham never rises higher than 14°, a high quality baseline and repeatable line profiles and line intensities were obtained. From the data, we have determined the line flux, $\int T_{\rm MB}{\rm d}v$, and we have estimated the line width and the radial velocity using either Gaussian fits to the lines, or, in the case of non-Gaussian lineshapes, giving the first or second moments of the spectra. Results as well as intensities of the $1 - 0$ and $2 - 1$ lines, which were observed by us or taken from published 30-m data, are given in Table 1. In Table 2, we summarize important source parameters together with the flux ratio of the ^{12}CO $3 - 2$ and $1 - 0$ lines.

In general, there is good agreement between shapes and intensities of our observed lines and other $J = 3 - 2$ data (see the Appendix). Data taken in April 1998 at our positions with the same setup (R. Wielebinski, pers. comm.) show virtually identical calibration scales for M 82, M 83, IC 342, NGC 2146, NGC 3351 and NGC 5907. For NGC 3627, NGC 3628 and M 51 these data show a 30% higher intensity, and for NGC 3079 a 30% lower intensity. Such differences are compatible with our estimate of the calibration errors and with the uncertainties from the fits to the line profiles.

Our literature search made clear that the application of correct calibration schemes cannot be taken for granted in all cases. In order to present a sample that is as homogeneous as possible, we therefore restrict our comparison to CO $1 - 0$ and $2 - 1$ data which have been measured using the IRAM 30-m telescope. In Fig. 2 we show the velocity integrated relative intensities of the three lowest CO transitions, normalized to the CO $1 - 0$ transition.

Table 2. Properties of the observed galaxies

Source	Type	$D^{\rm b}$ Mpc	$L^{\rm a}_{\rm IR}$ $10^9{\rm L}_\odot$	$T^{\rm a}_{\rm Dust}$ K	$\frac{I_{32}}{I_{10}}$
IC 10	IBm	0.82			.1
NGC 253	SAB(s)c	2.5	13	42.7	1.1[c]
NGC 891	SA(s)b	9.6	19	28.7	.21
Maffei 2	SAB(rs)bc	2.3			1.1
IC 342	SAB(rs)cd	1.8	0.9	38.7	.66
NGC 2146	SB(s)ab pec	17	110	40.7	1.6
NGC 2903	SAB(rs)bc	6.3	6.5	32.0	.68
NGC 2964	SAB(r)bc	22	21	35.0	.68
M 82	I0	3.2	32	46.5	1.1
NGC 3079	SB(s)c	20	62	35.3	.68
NGC 3227	SAB(s) pec	21	15	33.6	.30
NGC 3351	SB(r)b	8.1	4.0	35.5	1.6
NGC 3368	SAB(rs)ab	8.1	2.8	30.2	.62
NGC 3627	SAB(s)b	6.6	8	32.0	.22
NGC 3628	SB pec	7.7	11	34.7	.24
NGC 4088	SAB(rs)bc	17	26	31.7	.44
NGC 4102	SAB(s)b	17	40	40.7	.36
NGC 4414	SA(rs)c	10	12	32.8	.67
NGC 4818	SAB(rs)ab	22	28	42.7	.47
NGC 5055	SA(rs)bc	7	8	28.3	.40
Cen A	S0 pec	5	16	35.5	
M 51	SA(s)bc pec	7.7	13	27.7	.62
M 83	SAB(s)c	4.7	9	34.2	
NGC 5907	SA(s)c	15	14	26.7	.19
Arp 220	S?	73	1300	46.2	.90
NGC 6000	SB(s)bc	30	96	39.7	.13
NGC 6217	(R)SB(rs)bc	24	21	36.9	.68
NGC 6946	SAB(rs)cd	5.2	7	30.8	.68
NGC 7331	SA(s)b	14	26	29.0	.46[c]
NGC 7541	SB(rs)BC pec	33	80	34.7	.25

[a] $T_{\rm dust}$ computed from the 60 and 100 μm IRAS fluxes and assuming an emissivity that is proportional to ν, $L_{\rm IR}$ using IRAS data.
[b] if not otherwise noted: Tully (1988); IC 10: Wilson et al. (1996); Maffei 2, IC 342: McCall (1989); NGC 6946: Karachentsew & Sharina (1997)
[c] From data obtained by Harrison et al. (1998) with the 30-m telescope and the Caltech Sub-mm Telescope.

4. Discussion

In Fig. 3 we correlate the dust temperature, $T_{\rm Dust}$, and the infrared luminosity, $L_{\rm IR}$, with the intensity ratio of the CO $3 - 2$

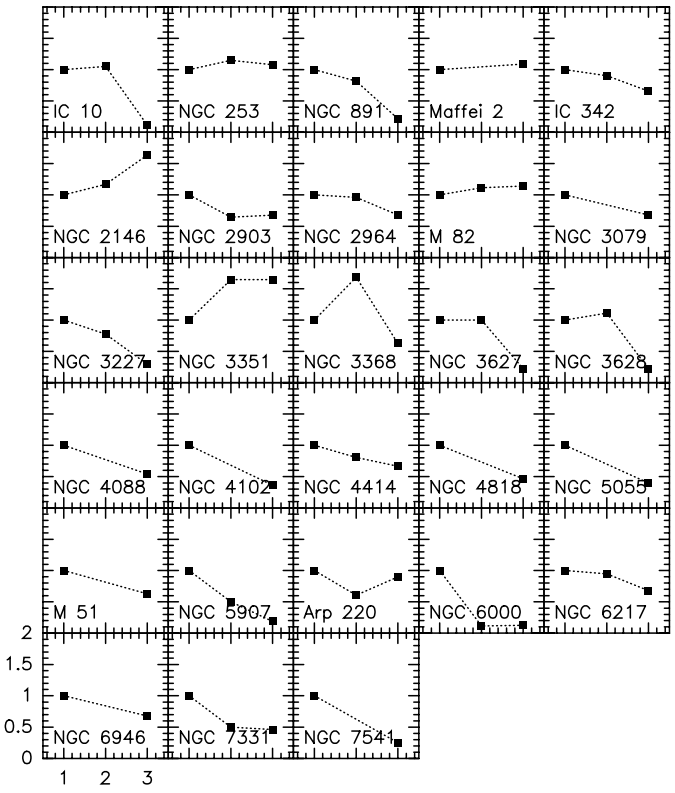

Fig. 2. The integrated intensity, $\int T_{\rm MB}{\rm d}v$ in K km s^{-1} of the three lowest CO lines. The $J = 1 - 0$ and $2 - 1$ data are from Braine et al. (1993) normalized to the $1 - 0$ line. For completeness, data from NGC 253 obtained at the IRAM 30-m telescope and the JCMT (Harrison et al., 1998) are also shown. All data refer to a beam of $\sim 21''$.

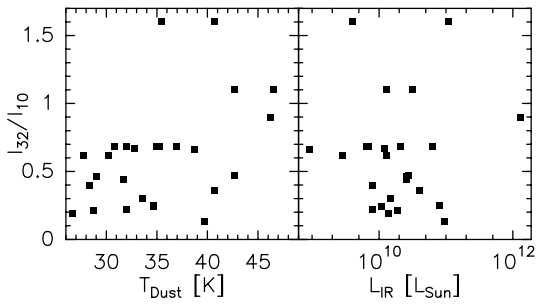

Fig. 3. Correlation between the dust temperature and IR luminosity with the intensity ratio of the CO $3-2$ and $1-0$ lines. The only sources which appear to have $I_{32}/I_{10} >> 1$ are NGC 2146 and NGC 3351.

and $1 - 0$ lines. The dust temperature was determined as explained in Table 2. The IR luminosity was extrapolated from the IRAS Point Source Catalog data using a scheme described in Wouterloot & Walmsley (1986). We also included data for NGC 253 measured by Harrison et al. (1998). It is evident that only a small fraction of the observed objects have intensity ratios I_{32}/I_{10} larger than 0.7. The objects with such a high ratio also have a high $T_{\rm Dust}$ in excess of 35 K and tend to have a higher IR luminosity. Among the rest of the sources there appears to

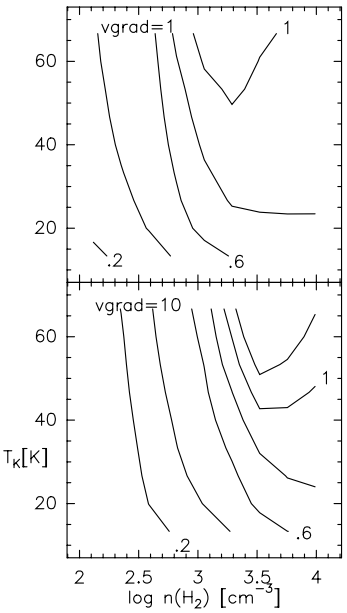

Fig. 4. As a result of model computations, the intensity ratios of the CO $3-2$ and $1-0$ lines are plotted as contours for a range of $T_{\rm kin}$ and $n({\rm H_2})$ for two values of the parameter $\frac{n({\rm CO})}{n({\rm H_2})}/\frac{{\rm d}v}{{\rm d}r}$, namely 10^{-4} and 10^{-5} $({\rm km\,s^{-1}/pc})^{-1}$, which corresponds to velocity gradients of 1 (upper panel) and 10 ${\rm km\,s^{-1}/pc}$ (lower panel) if the relative abundance of CO is 10^{-4}.

be no correlation between $T_{\rm dust}$ or $L_{\rm IR}$ and I_{32}/I_{10}, the value of which scatters between 0.2 and and 0.7.

There are several caveats in interpreting the diagrams in Fig. 3. First, many nearby galaxies are extended with respect to our beam and even with respect to the much larger (1′) IRAS beam. As a consequence, the CO measurements may reflect conditions in a more active nuclear region than the IRAS data. Since, however, IRAS fluxes are biased toward a warm dust component, which may also arise from a compact central region, comparing properties derived from IRAS data with those from CO measurements need not be a problem. Second, with increasing distance, the ratio I_{32}/I_{10} should decrease, as more radiation from lesser excited CO lines arising from the disk regions is picked up by the beam. This may be partly compensated if the more distant sources of our sample (which tend to be more luminous) also have a larger fraction of highly excited gas.

We have performed computations of the radiative transfer and excitation of CO for a range of kinetic temperatures and H_2 densities using the large velocity gradient approximation for a spherical molecular cloud. Collision rates are taken from De Jong et al. (1975). The model used is described in Henkel et al. (1980). We took $\frac{n({\rm CO})}{n({\rm H_2})}/\frac{{\rm d}v}{{\rm d}r} = 10^{-4}$ and 10^{-5} $({\rm km\,s^{-1}/pc})^{-1}$. The results of these computations can be found in Fig. 4.

It is evident that for the input parameters used, I_{32}/I_{10} can only become unity or higher if the gas temperatures are $\gtrsim 50$K and average H_2 densities, $n({\rm H_2})$, exceed 10^3 cm^{-3}. For a temperature range of 20 to 60 K, the intensity ratio is mainly related to $n({\rm H_2})$: a ratio of 0.2 would indicate densities of $< 300\,{\rm cm^{-3}}$ and a ratio as high as 0.6 indicates densities in the range of

$1000\,\mathrm{cm}^{-3}$. In most cases the $3-2$ line is less intense than lower lying lines. Line intensity ratios close to unity are found toward the prominent starburst galaxies NGC 253, M 82 and Arp 220 indicating high densities and temperatures for a large fraction of the molecular gas in the beam. There are only few sources where the $3-2$ line is stronger than the $1-0$ line. Among those is NGC 2146 where I_{32}/I_{10} is as high as to 1.6. This behavior is expected for optically thin CO lines from warm gas, which seems to be exceptional.

Optical depths and thus the velocity gradient could be estimated best from observations of rare isotopic substitutions of CO. Güsten et al. (1993) pointed out that in many galaxies there exist several molecular components with different temperatures and densities and demonstrated that observations of isotopic CO lines and of higher transitions of CO will allow us to better constrain the range of possible physical parameters. The next CO line which can be observed from the ground, the CO $J=4-3$ line, is 55 K above the ground level. Our observations clearly indicate that this line can be observed in many sources.

5. Conclusions

The main conclusions of this paper are:

1. We have searched for the $J=3-2$ line of ^{12}CO toward 29 external galaxies and have detected emission from all of them. For most sources these are the first published sub-mm CO line data. The good quality of the baselines and the high signal-to-noise ratios demonstrate the suitability of the Heinrich-Hertz-Telescope for extragalactic sub-mm observations.
2. For most sources, the I_{32}/I_{10} ratios are in the range 0.2–0.7. This implies that it is possible to detect this line in hundreds of galaxies, to investigate the spatial structure of prominent sources, and to study the excitation conditions by observing isotopic CO lines and higher rotational lines.
3. Model calculations show that the I_{32}/I_{10} line ratio is an indicator of the average H_2 density in the regions observed. Observations of rare isotopic CO are needed for more exact evaluations.
4. Carefully calibrated and pointed mm-line data of M 82 show that the $2-1/1-0$ ratio is close to unity, falsifying an often cited legend about a ratio much higher than one.

Acknowledgements. We thank the staff at the Heinrich-Hertz-Telescope for their enthusiastic support. Dr. W. Peters made available data of the pointing behavior of the telescope. The director of the SMTO, Dr. T. L. Wilson, made available observing time at the HHT. Dr. D. Muders and A. Nicol helped to observe a CO $3-2$ spectrum of M 82. We thank Dr. R. Wielebinski for helpful discussions on the calibration and access to unpublished data. R.M. was supported by a Heisenberg fellowship by the DFG and by NATO grant SA.5-2-05 (CRG. 960086) 318/96 and thanks the MPIfR for its hospitality.

Appendix A: Notes on individual sources

IC 10. The observed position is the origin of a strong water maser (Henkel et al., 1986). Here, the $3-2$ line is much weaker than $1-0$ in the $21''$ beam of the 30-m telescope (Becker, 1990). CO $3-2$ has been recently observed by Petitpas & Wilson (1998). For two positions they report $(3-2)/(1-0)$ ratios of 0.3–0.5, which is slightly higher than the line ratio we find at a different position.

Maffei 2. This galaxy has been mapped in CO $1-0$ by Weliachew et al. (1988) with $23''$ resolution and in the $3-2$ line by Hurt et al. (1993) with a resolution of $22''$. Our spectrum shows the characteristic double profile, which is also seen in other transitions. There seem to be inconsistencies in the paper by Hurt et al. (1993) concerning their calibration, which also should influence their conclusions: While they claim that the $J=(3-2)/(1-0)$ ratio inferred from the data of Weliachew et al. (1988) is close to unity, Fig. 5 of Hurt et al. (1993) suggests a value closer to 2. If our calibration is correct, the $J=3-2/1-0$ intensity ratio is close to unity.

IC 342. There have been numerous molecular line observations of this nearby spiral. Observations of interstellar ammonia (Martin & Ho (1986)) suggest a kinetic temperature $\gtrsim 60\,\mathrm{K}$. An HCN map by Downes et al. (1992) shows a number of dense clumps of typically 20–30 pc in diameter. The free-free emission is mainly associated with clump B. Our observation of the ^{12}CO $J=3-2$ line was taken toward this clump. The integrated intensity measured by us ($138\,\mathrm{K\,km\,s^{-1}}$) is within the estimated calibration errors of published CO $J=3-2$ measurements (Irwin & Avery 1992: $111\,\mathrm{K\,km\,s^{-1}}$ in a $15''$ beam, Steppe et al. 1990: $165\,\mathrm{K\,km\,s^{-1}}$ within a convolved beam of $19''$, Wall et al. 1991: $139\,\mathrm{K\,km\,s^{-1}}$ in a $15''$ beam).

NGC 2146. We have used the same coordinates as Braine et al. (1993) and as Devereux et al. (1994). Our line shape resembles that of Braine et al. obtained with a $23''$ beam in the CO $J=2-1$ and $1-0$ lines. Devereux et al. (1994) observe a much smaller linewidth in the $3-2$ and $1-0$ line with a $14''$ beam. We are probably seeing a more extended gas component than Devereux et al. (1994), or there is a mispointing in the Devereux et al. data.

M 82 (NGC 3034). In the past, there have been claims of CO $(2-1)/(1-0)$ ratios of ~ 2 toward the center of M 82 due to optically thin CO emission. In Fig. A1, we show the profiles of the first three transitions of ^{12}CO convolved to a $21''$ beam. Line intensity ratios are close to one. The $1-0$ and $2-1$ profiles were produced from simultaneously made 5×5 point maps with $5''$ spacing. The IRAM data were shifted so that the profiles matched the profiles of the $3-2$ line. This was achieved at a nominal $\Delta\alpha = 5''$ for the $2-1$ line and $3''$ for the $1-0$ line. Note that due to the steep velocity gradients in the central region of M 82 the profile changes drastically with position shifts of just 2 or $3''$. This has to be borne in mind when comparing data from different telescopes or different transitions or molecules. Like in other starburst galaxies, we find $2-1/1-0$ and $3-2/1-0$ intensity ratios close to unity.

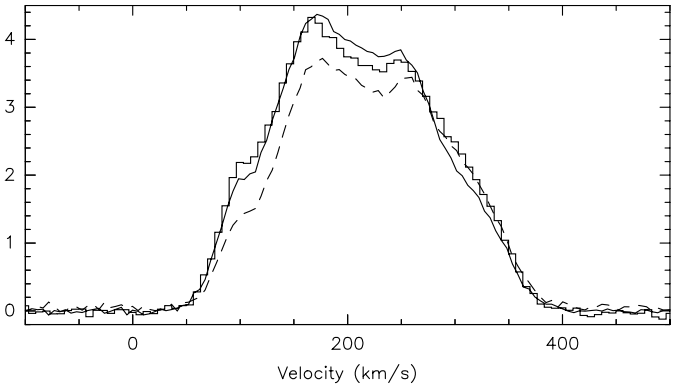

Fig. A1. The $J = 1 - 0$ (dashed lines), $2 - 1$ (solid lines) and $3 - 2$ (histogram) profiles of ^{12}CO toward the center of M 82. All spectra were convolved to a beam size of $21''$ and the nominal origins of the $1 - 0$ and $2 - 1$ profiles were shifted slightly until their shape matched that of the $3 - 2$ line. The temperature scale is $T_{\rm MB}$.

NGC 3351 (M 95). The line shape of the $3-2$ line is much more asymmetrical than that of the $2 - 1$ and $1 - 0$ spectra by Braine et al. (1993), indicating a possible mispointing of our data. The CO profiles exhibit a pronounced double peak. The blue-shifted peak at 700 km s^{-1} is much stronger in CO $3 - 2$ than in lower lying CO transitions. This indicates that it arises off-center perhaps coinciding with an optical ring (Jackson et al., 1989).

NGC 3627 and NGC 3628. The positions measured are offset from the central positions. Intensities of the $1 - 0$ and $2 - 1$ lines are taken at our $3 - 2$ positions from the maps by Reuter et al. (1991, 1996). CO $3 - 2$ intensities toward the centers of the galaxies are ~ 3 times higher than at the positions observed by us (R. Wielebinski, priv. comm.).

NGC 4818. With a $14''$ beam, Devereux et al. (1994) observed an integrated intensity, $\int T_{\rm MB}{\rm d}v$, of 60 K km s^{-1} in the $3 - 2$ line, while we see only 20 K km s^{-1} in our $21''$ beam. Presumably, the source we are observing is small compared to our beam, or there are pointing deviations.

Cen A (NGC 5128). This elliptical galaxy contains a dust lane, which is also seen in CO. Toward the center, many molecular lines are seen in absorption. We do see emission, but no signs of absorption as in the CO $3 - 2$ spectrum by Israel et al. (1991). This is due to the fact that we were using the coordinates in Paglione et al. (1997) which are offset from the continuum source by $(\Delta\alpha, \Delta\delta) = (16'', 9'')$, about one beam width off-center. Our profile looks similar to that of ^{13}CO $J = 1-0$ taken with the SEST at that position (Wild et al., 1997).

M 51 (NGC 5194). The spectrum was observed toward the dynamic center of M 51. The integrated intensity is comparable to that of the $J = 2 - 1$ line (García-Burillo et al., 1993). I_{32}/I_{10} ratios close to 1 were found toward many off center positions of this spiral (Bash et al., 1990).

M 83 (NGC 5236). This galaxy has been mapped by Handa et al. (1990) with a $16''$ beam in the CO $1 - 0$ line. The lineshape is in good agreement with our data.

Arp 220 (IC 4553/4). The CO $3 - 2$ line is similar in intensity to the $1 - 0$ line measued by Radford et al. (1991). It is also consistent with the CO $2 - 1$ in Rigopoulou (1996). Note that the intensities in Table 2 of that publication are given in antenna temperature and not, as stated, in main-beam brightness temperature (D. Rigopoulou, priv. comm.). However, the $3 - 2$ line is double peaked, whereas the $1 - 0$ and $2 - 1$ lines from filled aperture observations show a single maximum. A recent interferometer map in CO $2 - 1$ also reveals a double peak structure arising from a compact ($\sim 2''$), molecular source (Scoville et al., 1997). Possibly the $1 - 0$ and $2 - 1$ single dish data trace a more smoothly distributed or more extended medium while the $3 - 2$ is mainly seen from fewer clumps with high excitation within the compact molecular disk. It is interesting that in our data the redshifted peak is of higher intensity than the blueshifted one, while in the Scoville et al. (1997) data the blueshifted peak is stronger. Whether this is an excitation effect or is just caused by the different spatial sampling can be decided by higher resolution observations of the CO $3 - 2$ line.

NGC 7331. The lineshape is different from that of CO $1 - 0$ and $2 - 1$, suggesting a pointing offset.

References

Baars J., Martin R.N., 1996, Rev. Modern. Astron. 9, 111
Bash F., Jaffe D., Wall W., 1990, Windows on galaxies, p. 227, ed.: G. Fabbiano et al., Kluwer
Becker R., 1990, Ph.D. thesis, Bonn University
Bitran M., Alvarez H., Bronfman L., May J., Thaddeus P., 1997, A&AS 125, 99
Boisse P., Casoli F., Combes F., 1987, A&A 173, 229
Braine J., Combes F., Casoli F. et al., 1993, A&AS 97, 887
Chini R., Krügel E., Lemke R., 1996, A&AS 118, 47
De Jong T., Dalgarno A., Chu S. I., 1975, ApJ 199, 69
Devereux N., Taniguchi Y., Sanders D. B., Nakai N., Young J. S., 1994, AJ 107, 2006
Downes D., 1989, Introductory Course in Galaxies Evolution and Observational Astronomy, p. 353, eds.: I. Appenzeller, H. Habing, P. Léna, Springer Verlag
Downes D., Radford S.J.E., Guilloteau S. et al., 1992, A&A 262, 424
Eckart A., Downes D., Genzel R. et al., 1990, ApJ 348, 434
Elfhag T., Booth R.S., Höglund B., Johansson L.E.B., Sandqvist A., 1996, A&AS 115, 439
García-Burillo S., Guélin M., Cernicharo J., Dahlem M. 1992, A&A 266, 21
García-Burillo S., Guélin M., Cernicharo J., 1993, A&A 274, 123
Güsten R., Serabyn E., Kasemann C. et al., 1993, ApJ 402, 537
Handa T., Nakai N., Sofue Y., Hayashi M., Fujimoto M., 1990, PASJ 42, 1

Harrison A., Henkel C., Russell A., 1998, MNRAS, in press
Henkel C., Walmsley C. M., Wilson T. L., 1980, A&A 82, 41
Henkel C., Wouterloot J. G. A., Bally J., 1986, A&A 155, 193
Hurt R.L., Turner J.L., Ho P.T.P., Martin R.N., 1993, ApJ 404, 602
Irwin J.A., Avery L.W., 1992, ApJ 388, 328
Israel F.P., Van Dishoeck E.F., Baas F., De Graauw T., Phillips T.G., 1991, A&A 245, L13
Israel F.P., White G.J., Baas F., 1995, A&A 302, 343
Jackson J.M., Eckart A., Cameron M. et al., 1991, ApJ 375, 105
Jackson J.M., Snell R.L., Ho P.T.P., Barrett A.H., 1989, ApJ 337, 680
Karachentsev I. D., Sharina M. E., 1997, A&A 324, 457
Martin R. N., Ho P. T. P., 1986, ApJ 308, L7
Mauersberger R., Henkel C., Whiteoak J. B., Chin Y. N., Tieftrunk A.R., 1996a, A&A 309, 705
Mauersberger R., Henkel C., Wielebinski R., Wiklind T., Reuter H.-P., 1996b, A&A 305, 421
McCall M.L., 1989, AJ 97, 1341
Paglione T.A.D., Jackson J.M., Ishizuki S., 1997, ApJ 484, 656
Petitpas G.R., Wilson C.D., 1998, ApJ 496, 226
Radford S.J.E., Downes D., Solomon P.M., 1991, ApJ 368, L15
Reuter H.-P., Krause M., Wielebinski R., Lesch H., 1991, A&A 248, 12
Reuter H.-P., Sievers A.W., Pohl M., Lesch H., Wielebinski R., 1996, A&A 306, 721
Rigopoulou D., Lawrence A., White G.J., Rowan-Robinson M., Church S.E., 1996, A&A 305, 747
Sage L.J., 1993, A&AS 100, 537
Scoville N.Z., Yun M.S., Bryant P.M., 1997, ApJ 484, 702
Solomon P.M., Radford S.J.E., Downes D., 1990, ApJ 348, L53
Steppe H., Mauersberger R., Schulz A., Baars J.W.M., 1990, A&A 233, 410
Strong A.W., Bloemen J.B.G.M., Dame T.M. et al. , 1988, ApJ 207, 1
Tilanus R., Tacconi L., Sutton E. et al., 1991, ApJ 376, 500
Tully B., 1988, Nearby Galaxies Catalog, Cambridge Univ. Press
Wall W.F., Jaffe D.T., Bash F.N., Israel F.P., 1991, ApJ 380, 384
Weliachew L., Casoli F., Combes F., 1988, A&A 199, 29
White G.J., Ellison B., Claude S., Dent W.R.F., Matheson D.N., 1994, A&A 284, L23
Wild W., Eckart A., Wiklind T., 1997, A&A 322, 419
Wilson C.D., Welch D.L., Reid I.N., Saha A., Hoessel J., 1996, AJ 111, 1106
Wouterloot J.G.A., Walmsley C.M., 1986, A&A 168, 237
Young J., Xie S., Tacconi L. et al., 1995, ApJS 98, 219